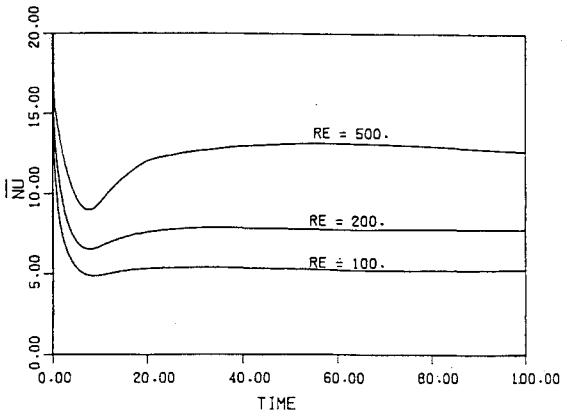

Fig. 6 The time-dependent average Nusselt numbers for Re = 100, 200, and 500.

Conclusion

A numerical solution has been obtained for the problem of transient laminar forced convection from a circular cylinder. The governing equations expressed in the body-fitted coordinates were solved numerically by the SADI method. The SADI method was applied to increase the accuracy, simplify the treatment of the boundary conditions, and save CPU time. The comparisons between the present results and previous investigation are found to be satisfactory.

References

[1]Thoman, D., and Szewczyk, "Time Dependent Viscous Flow Over a Circular Cylinder," *Physics of Fluids*, Suppl. II, 1969, pp. 79–86.

[2]Gresho, P. M., Lee, R. L., and Sani, R. L., "On the Time-Dependent Solution of the Incompressible Navier-Stokes Equations." *Recent Advances in Numerical Methods in Fluids*, Pineridge Press, Swansea, 1980, pp. 27–80.

[3]Hwang, R. R., Chiang, T. P., and Chiao, M. T., "Time-Dependent Incompressible Viscous Flow Past a Circular Cylinder," *Journal of Chinese Institute of Engineering*, Vol. 9, 1986, pp. 617–631.

[4]Jordan, S. K., and Fromm, J. E., "Oscillatory Drag, Lift, and Torque on a Circular Cylinder in a Uniform Flow," *Physics of Fluids*, Vol. 15, 1972, pp. 371–376.

[5]Lin, C. L., Pepper, D. W., and Lee, S. C., "Numerical Methods for Separated Flow Solutions Around a Circular Cylinder," *AIAA Journal*, Vol. 14, 1976, pp. 900–907.

[6]Patel, V. A., "Karman Vortex Street Behind a Circular Cylinder by the Series Truncation Method," *Journal Computational Physics*, Vol. 28, 1978, pp. 14–42.

[7]Lecointe, Y., and Piquet, J., "On the Use of Several Compact Methods for the Study of Unsteady Incompressible Viscous Flow Around a Circular Cylinder," *Computational Fluids*, Vol. 12, 1984, pp. 255–280.

[8]Smith, S. L., and Brebbia, C. A., "Improved Stability Techniques for the Solution of N-S Equations," *Applied Mathematical Modeling*, Vol. 1, 1977, pp. 227–234.

[9]Jain, P. C., and Goel, B. S., "A Numerical Study of Unsteady Laminar Forced Convection from a Circular Cylinder," *Journal of Heat Transfer*, 1976, pp. 303–307.

[10]McAdam, W. H., *Heat Transmission*, McGraw-Hill, New York, 1954.

[11]Kramers, H. A., "Heat Transfer From Sphere to Flowing Media," *Physics*, Vol. 12, 1946, pp. 61–80.

[12]Van der Hegge Zijnen, B. G., *Applied Science Research*, Vol. A6, 1956, pp. 129.

[13]Tsubouchi, T., and Masuda, A. H., Rept. No. 191, Institute of High Speed Mechanics, Tohoku Univ., Japan, 1966.

[14]Karniadakis, G. E. M., "Numerical Simulation of Forced Convection Heat Transfer from a Cylinder in Crossflow," *International Journal of Heat Mass Transfer*, Vol. 31, No. 1, 1988, pp. 107–118.

[15]Rubin, S. G., and Graves, R. A., "Viscous Flow Solution with a Cubic Spline Approximation, Computers and Fluids," Vol. 3, 1975, pp. 1–36.

[16]Thompson, J. F., Thames, F. C., Mastin, C. W., and Shanks, S. P., "Use of Numerically Generated Body-Fitted Coordinate Systems for Solution of the Navier-Stokes Equations," *Proceeding of the AIAA 2nd Computational Fluid Dynamics Conference*, Hartford, CT, 1975.

Electron Temperature and Electron Density in a Rarefied Air Plasma Jet

M. A. Dudeck,* P. Lasgorceix,† C. Voisin,‡ and S. Cayet§
Centre National de la Recherche Scientifique, Meudon 92190, France

Introduction

AIR jets at low pressure and high temperature are used to simulate some properties of the gas layer surrounding a spacecraft while re-entering the atmospheric zone. Various experimental setups have been developed in order to realize these jets. Hypersonic simulations at low pressure are obtained in wind tunnels[1] working continuously or transient wind tunnels, to measure force, flow, surface temperature, and turbulence. During a re-entry, real gas effects appear between the shock wave and the surface. It concerns especially chemical, ionization, and vibrational nonequilibrium effects. Some of these effects can be studied in air by shock tubes[2–4] or by microwave discharge techniques[5,6] and by arc jets.[7–10] Arc jets can be used to obtain a stationary and large plasma jet arc, but the main difficulty in producing arc jets in a wind tunnel lies in the destruction of electrodes due to the presence of oxygen. A solution may be obtained by injecting oxygen into the nozzle, after the arc.[8,10] This paper presents a generator that produces steady plasma arc jets directly from air for about 1 h at a pressure of 0.08 Torr. Radial profiles of temperatures and densities measured by an electrostatic probe are shown. Electrostatic probe method gives electron density and electron temperature with a good spatial resolution and a characteristic time function of the frequency of the probe potential. Difficulties may appear in the analysis of the probe characteristic, total current collected by the surface probe as a function of probe potential (fluctuations, theory). Electrostatic probes have been used in different types of air plasmas. Single-electrode Langmuir probe measurements have been performed in air at a static pressure of 30 Torr to study the electron attachment by the addition of small quantities of an electrophilic gas.[8] Spherical double probes[6] have been used in air plasma generated by microwaves (900 MHz) in the pressure range 1–10 Torr. The ion density has been measured in air shock tube at initial pressure of 0.075–1.2 Torr by a hollow electrostatic probe at a large negative potential.[5] A thin-wire Langmuir probe[2] has been used in shock tunnel flows to determine the electron density and the electron temperature to deduce the reaction rate coefficient for the reaction $NO^+ + e$. A set of tungsten electrostatic probes has been tested[3] in a hypersonic shock tunnel flow to perform analyses in air. The effects of the probe length, diameter, ratio of probe radius to Debye length, angle of attack, and length-to-diameter ratio are studied. In an arc-heated shock tube at initial pressures 0.1 and 1 Torr, the ion saturation currents have been measured in air with flush electrostatic probes.

Received Oct. 27, 1989; revision received Dec. 31, 1990; accepted for publication Jan. 2, 1991.

*Professor, Laboratoire d'Aérothermique du CNRS, 4ter, Route des Gardes.

†Research Scientist, Laboratoire d'Aérothermique du CNRS, 4ter, Route des Gardes.

‡Research Engineer, Laboratoire d'Aérothermique du CNRS, 4ter, Route des Gardes.

§Graduate Student, Laboratoire d'Aérothermique du CNRS, 4ter, Route des Gardes.

Experimental Apparatus

Air plasma experiments are performed in a cylindrical vacuum chamber (SR 5), 1.5 m long and 1 m in diameter (Fig. 1). Vacuum conditions are obtained by a pumping set providing a volume flow rate of 20,000 $m^3\ h^{-1}$ at a pressure of 5×10^{-2} Torr.

The plasma generator uses a copper cathode with a zirconium insert (Fig. 2). This insert is 1.5 mm in diameter and the copper cathode is water-cooled. A helicoid screw forces a rotational motion on the air around the cathode. The anode is the neck of the copper nozzle and is also water-cooled. The neck is 4 mm in diameter, the divergent angle of the nozzle is 60 deg, and the anode-cathode spacing is 4 mm. Electrodes are connected by a power supply with adjustable current. An arc discharge is initiated by a high-frequency, high voltage (1 MHz, 4000 V) electric shock between the cathode and the neck nozzle. The current is regulated to 100 A before starting the arc discharge. Figure 3 shows the current-voltage characteristic for an arc intensity between 35 and 130 A. In this intensity range, the electric power varies as a linear function from 2.4 to 7 kW (±7%).

Electron Temperature and Electron Density

The air mass flow rate for the above test is 15 standard liters per minute (with air, 1 standard liter per minute = 0.0215 $g.s^{-1}$). The arc intensity remains constant at 100 A and the static pressure in the wind tunnel is 0.08 Torr. Plasma jets are steady, cylindrical in symmetry, and without wall interactions. They are 50 cm maximum in diameter. The same cathode is sufficient for 1-h experiments. The evaporated zirconium mass is negligible compared to the air mass injected into the generator (10^{-5} in ratio).

The electron temperature and the electron density are measured with a pulsed electrostatic probe. This probe is made with a tungsten rod 2 mm in diameter coated with an alumina deposited on the lateral surface. Only the flat end of the rod is in contact with the plasma. The probe axis is perpendicular to the plasma flow velocity. The probe is connected to a generator which delivers a triangular potential with a variable frequency. For those tests, we assume a frequency of 100 Hz. For each measurement, five probe characteristics are superposed and converted by a digitizing oscilloscope to obtain 1016 points. These points are then analyzed by a computer. The Langmuir theory, admitting a noncollisional potential sheath around the probe, is used to analyze the characteristic. To determine the electron temperature, the following relation is used:

$$T_e = -\frac{e}{k}\frac{dV}{d(\ln I_e)}$$

where e is the charge of electron, k is the Boltzmann's constant, V is the probe potential, and I_e is electron current. In order to obtain a good estimation of T_e, the slope $d \ln I_e/dV$ is computed by the mean square method using 30 successive points $\{V_n, \ldots, V_{n+29}\}$ for $n = 1, \ldots$. Electron temperature is deduced from the value of the current at the plasma potential.

Figure 4 presents a radial profile of the electron density measured at a distance of 50 cm from the nozzle outlet. The maximum density on the jet axis is 6.6×10^{10} cm^{-3}. The maximum electron temperature is about 4700 K. At a distance of 15 cm from the jet axis, the electron temperature is about 4000 K (Fig. 5). The value of electron density obtained by electrostatic probe method in air plasma appears to comply

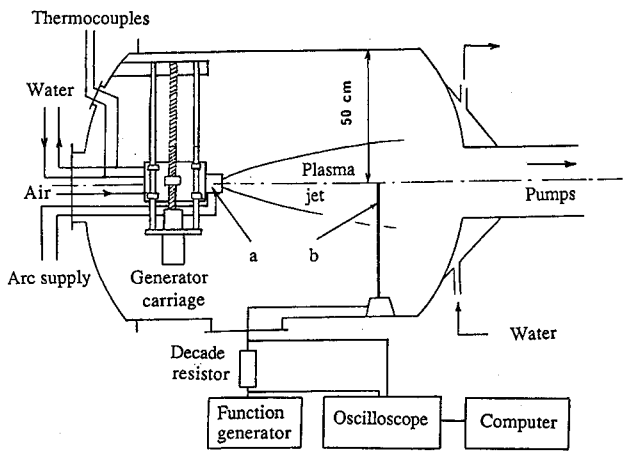

Fig. 1 Wind tunnel: *a*, Plasma generator; *b*, single electrostatic probe.

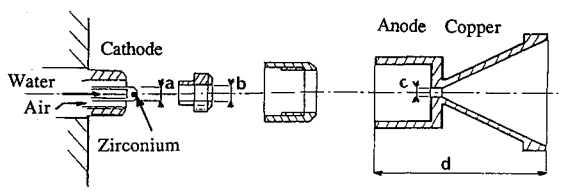

Fig. 2 Plasma generator: *a*, 6 mm; *b*, 7 mm; *c*, 4 mm; *d*, 78 mm.

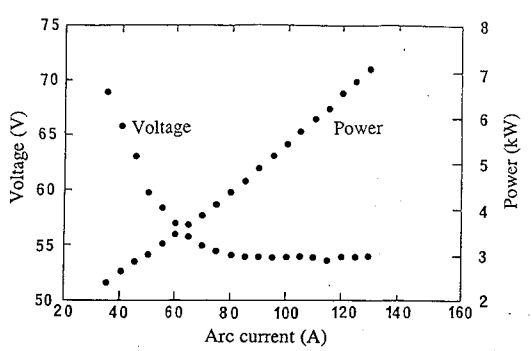

Fig. 3 Arc voltage and electric power as a function of the arc current.

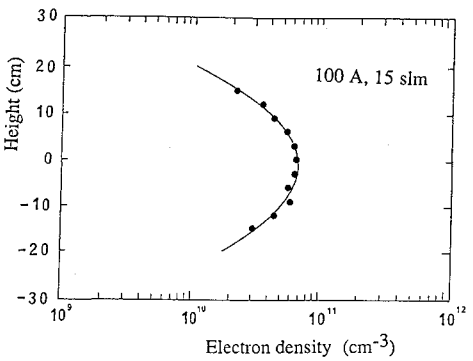

Fig. 4 Radial profile of the electron density. The height is measured from the plasma axis.

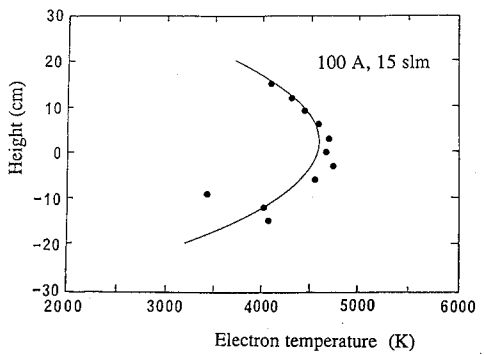

Fig. 5 Radial profile of the electron temperature.

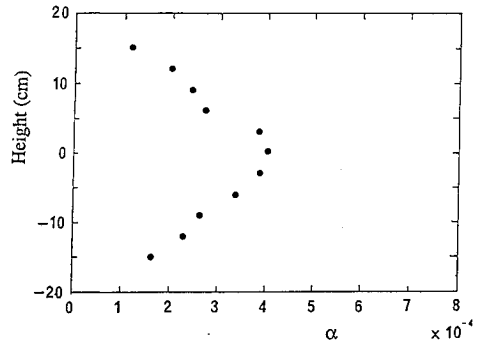

Fig. 6 Radial profile of the ion fraction.

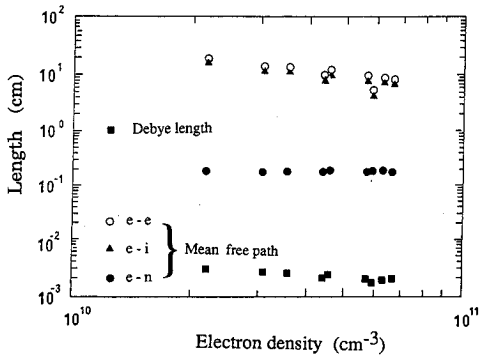

Fig. 7 Characteristic lengths of the plasma as a function of the electron density.

with precedent results by hyperfrequency propagation (2.45–5 GHz) in a boundary layer on a flat plate.

The theory associated with the noncollisional potential sheath is justified if the energy distribution for the electrons is a Maxwellian function, and if the shortest mean free path is much larger than the Debye length. Exponential increase noticed for the current collected by the sensitive part of the probe leads to the assumption of a Maxwellian distribution function for electron energy.

Using the assumption of a thermal local equilibrium between the electron temperature and the translational temperature of heavy species and using the measured static pressure, the ion fraction α of the plasma is evaluated from the relation $\alpha = n_e kT_e/p$. For the measurements made, the ionization fraction is about 10^{-4} (4×10^{-4} on the axis and 10^{-4} at 15 cm from the axis) (Fig. 6). Various mean free paths have been calculated with formulas expressing electron–ion, electron–electron, and electron–neutral collision frequencies:

$$\nu_{e-i}(s^{-1}) = 2.4\ 10^{-5} * n_e(\mathrm{cm}^{-3}) * T_e(eV)$$

$$\nu_{e-e}(s^{-1}) = 0.85 * \nu_{e-i}$$

$$\nu_{e-n}(s^{-1}) = 4\ 10^{9} * p(\mathrm{Torr}) * (T_e(eV))^{1/2}$$

eV: electron-volt.

The electron temperature and electron density show that the Debye length is always much shorter than the electron–neutral mean free path, which is the shortest among the three (Fig. 7). The assumption of a noncollisional path potential sheath is then justified.

The described plasma generator is used to obtain ionized air jets without using an oxygen injection into the plasma either straight in the jet, or close to the neck of the nozzle. The electron characteristics in density and temperature, as well as the pressure and jet stability, make the ionized gas obtained interesting to study for atmospheric re-entry problems. The ionic composition of jets obtained will be analyzed by a quadripolar mass spectrometer.

References

[1]"Technical Evaluation Report on Fluid Dynamics," Panel Symposium on Aerodynamics of Hypersonic Lifting Vehicles, AGARD-AR-246, 1988.

[2]Dunn, M. G., and Lordi, J. A., "Measurement of Electron Temperature and Number Density in Shock-Tunnel Flow," *AIAA Journal,* Vol. 7, No. 11, 1969, pp. 2099–2104.

[3]Lederman, S., Bloom, M. H., and Widhopf, G. F., Experiments on Cylindrical Electrostatic Probes in a Slightly Ionized Hypersonic Flow," *AIAA Journal,* Vol. 6, No. 11, 1968, 2133–2139.

[4]Scharfman, W. E., and Bredfeldt, H. R., "Experimental Investigation of Flush-Mounted Electrostatic Probes," *AIAA Journal,* Vol. 8, No. 4, 1970, pp. 662–665.

[5]Thompson, W. P., and de Boer, P. C. T., "Ion Density Measurements with an Electric Probe," *AIAA Journal,* Vol. 13, No. 8, 1975, pp. 1115–1117.

[6]Dorman, F. H., and Hamilton, J. A., "Double Probes in a Slightly Ionized Collisional Plasma," *International Journal of Mass Spectrometry and Ion Physics,* Vol. 20, No. 4, 1976, pp. 411–424.

[7]Blackwell, H. E., Yuen, E., Arepalli, S., and Scott, C. D., "Nonequilibrium Shock Layer Temperature Profiles from Arc Jet Radiation Measurements," AIAA Paper 89-1679, Buffalo, NY, June 1989.

[8]Starner, K. E., "Evaluation of Electron Quench Additives in a Subsonic Air Arc Channel," *AIAA Journal,* Vol. 7, No. 12, 1969, pp. 2357–2358.

[9]Lasgorceix, P., Dudeck, M. A., Caressa, J. P., "Measurements in Low Pressure, High Temperature and Reaction Nitrogen Jets," AIAA Paper 89-1919, Buffalo, NY, June 1989.

[10]Messerschmid, E., "Characterization of IRS Plasma Jet," Hermès Plasma Diagnostics Meetings, Stuttgart, RFA, Nov. 25, 1987.

Radiative Transfer in Multidimensional Enclosures with Specularly Reflecting Walls

A. S. Jamaluddin* and W. A. Fiveland†
Babcock & Wilcox, Alliance, Ohio 44601

Introduction

RADIATION is the dominant heat transfer mechanism in most large-scale industrial applications. The efficiency of radiative transfer depends on the boundary conditions, e.g., the temperature and the emissivity of the surrounding walls, and the target where heat transfer is desired. Previous studies[1-3] have shown that radiative transfer is highly sensitive to the wall emissivity.

In most heat transfer calculations, the walls are assumed to be diffusely reflecting. In some practical applications, however, the wall reflectivity may be partially specular. Industrial furnaces used for drying paint are an example of furnaces with partially specular walls.

The present work studies the effect of a specular component of reflectivity on wall radiative flux. The reflectivities, defined as $(1 - \epsilon)$ for an opaque surface, are segmented into diffuse and specular components, and the S_n discrete-ordinates method is employed to obtain solutions of the radiative transfer equation. An S_4 approximation is used, since higher order ap-

Presented at the AIAA/ASME 5th Joint Heat Transfer Conference, Seattle, WA, June 18–20, 1990; received June 25, 1990; revision received Jan. 24, 1991; accepted for publication Jan. 24, 1991.

*Senior Research Engineer, Alliance Research Center; currently, with Shell Development Co., P.O. Box 1380, Houston, TX 77251-1380.

†Group Supervisor, Alliance Research Center.